

Lawrence Berkeley National Laboratory

LBL Publications

Title

Nematic superconductivity stabilized by density wave fluctuations: Possible application to twisted bilayer graphene

Permalink

<https://escholarship.org/uc/item/0nf178h4>

Journal

Physical Review B, 99(14)

ISSN

2469-9950

Authors

Kozii, Vladyslav

Isobe, Hiroki

Venderbos, Jörn WF

et al.

Publication Date

2019-04-01

DOI

10.1103/physrevb.99.144507

Peer reviewed

Nematic superconductivity stabilized by density wave fluctuations: Possible application to twisted bilayer graphene

Vladyslav Kozii,¹ Hiroki Isobe,¹ Jörn W. F. Venderbos,^{2,3} and Liang Fu¹

¹*Department of Physics, Massachusetts Institute of Technology, Cambridge, MA 02139, USA*

²*Department of Physics and Astronomy, University of Pennsylvania, Philadelphia, Pennsylvania 19104, USA*

³*Department of Chemistry, University of Pennsylvania, Philadelphia, Pennsylvania 19104, USA*

Nematic superconductors possess unconventional superconducting order parameters that spontaneously break rotational symmetry of the underlying crystal. In this work we propose a mechanism for nematic superconductivity stabilized by strong density wave fluctuations in two dimensions. While the weak-coupling theory finds the fully gapped chiral state to be energetically stable, we show that strong density wave fluctuations result in an additional contribution to the free energy of a superconductor with multicomponent order parameters, which generally favors nematic superconductivity. Our theory sheds light on the recent observation of rotational symmetry breaking in the superconducting state of twisted bilayer graphene^{1,2}.

PACS numbers: 74.20.Rp, 74.20.Mn, 74.45.+c

I. INTRODUCTION

Unconventional superconductors can have multicomponent superconducting order parameters which transform in a multidimensional representation of the crystal symmetry group. In such cases, additional symmetries besides the $U(1)$ gauge symmetry — such as time-reversal or rotation symmetry — are broken in the superconducting state. Superconductors which break rotation symmetry can be called nematic superconductors (NSC), in analogy with rotational symmetry breaking in liquid crystals, whereas superconductors which break time-reversal symmetry are known as chiral superconductors. Nematic and chiral superconducting order parameters that belong to the same multiplet are degenerate at the superconducting transition temperature, while this degeneracy is lifted at lower temperature.

Recently, NSC have attracted a lot of attention following the discovery of rotation symmetry breaking in superconducting states of doped topological insulators Bi_2Se_3 in Knight shift³, upper critical field^{4–8}, specific heat^{4,5}, magnetic torque⁹ and STM¹⁰ measurements. Importantly, no signatures of rotational symmetry breaking were found in the normal state, indicating that nematicity is a property of the superconducting state itself. The observed features are consistent with a nematic superconductor with a two-component odd-parity SC order parameter^{11,12}.

The studies of NSC have mainly focused on strongly spin-orbit-coupled 3D materials and have considered odd-parity pairings^{13–25}. As shown by weak-coupling approach^{13,14}, in the presence of strong spin-orbit coupling and odd-parity pairing, the nematic superconducting state can be energetically more favorable than the chiral one due to the difference in their gap structures. In contrast, for two-dimensional (2D) systems without spin-orbit coupling, NSC is not expected from the gap structure: In 2D, the chiral $p + ip$ or $d + id$ SC states generally have a full superconducting gap on the Fermi

surface, whereas the nematic p_x (p_y) or $d_{x^2-y^2}$ (d_{xy}) states have point nodes. As a result, the chiral state has a lower energy compared to the nematic state within a weak-coupling treatment^{26–30}.

In this work, we propose a mechanism for p - or d -wave nematic superconductivity in 2D systems with hexagonal symmetry D_6 . We focus on the vicinity of the superconducting transition temperature, which allows us to treat the problem within the Ginzburg-Landau (GL) theory. By going beyond the weak-coupling approach which only takes into account the energy of Bogoliubov quasiparticles, we show that sufficiently strong fluctuations of a density wave order stabilize the NSC. The energy of such fluctuations is affected by the presence of a pairing potential and can thus distinguish between different SC states. Usually, the corresponding contribution is small compared to the weak-coupling term; however, it becomes more significant as the strength of fluctuations grows. This effect is known as a feedback mechanism and was originally proposed by Anderson and Brinkman to explain the stability of nodal A -phase in superfluid He-3 due to strong ferromagnetic fluctuations^{31–33}.

We show that strong density wave fluctuations generically favor nematic superconductivity in 2D. Our results are largely independent of microscopic details of such fluctuations. We find that the nematic d -wave state is stabilized more significantly by charge density wave (CDW) fluctuations, while the feedback contribution from spin density wave (SDW) is partially suppressed by the destructive interference in a coherence factor. Interestingly, the conclusion is dual in a case of two-component spin-triplet superconductivity, i.e., nematic p -wave SC is more stabilized by SDW. We emphasize that our analysis is valid not far from the superconducting transition point, where GL theory is applicable.

Our work is motivated by recent experiments on twisted bilayer graphene (TBG), which observed superconductivity and strongly correlated insulating state at 'magic' angle $\theta \approx 1.1^\circ$ ^{1,34,35}. The mechanism for su-

perconductivity in TBG and the pairing symmetry are subject to intense theoretical study^{36–62}. In particular, Ref. 36 showed that due to the Fermi surface nesting and the proximity to Van Hove singularity, unconventional superconductivity and density wave emerge as the two leading instabilities driven by Coulomb interaction. The most divergent superconducting instabilities are found in the two-component p -wave and d -wave superconducting channels, which are nearly degenerate when the intervalley exchange interaction is small. Related results on superconductivity from density wave/antiferromagnetic fluctuations in graphene superlattices appear in Refs. 37–39 (which propose chiral $p + ip$ and $d + id$ pairings). We thus expect that our strong-coupling theory of nematic superconductivity from density wave fluctuations is directly applicable to TBG. The strength of density wave fluctuations, which are important for our theory, may be enhanced by, e.g., changing electron density or tuning the twist angle and the interlayer spacing. We predict that one can observe the transition between chiral and nematic p/d -wave superconducting states upon varying these parameters.

Our result sheds light on the most recent measurements of in-plane upper critical magnetic field in TBG, which shows a pronounced two-fold anisotropy revealing the breaking of rotational symmetry². This experimental finding suggests the possibility of nematic p -wave or d -wave superconductivity, instead of chiral $p + ip$ or $d + id$ states which are isotropic. We emphasize that in our study nematicity is an intrinsic property of the anisotropic superconducting state, and we assume there is no primary electronic order that breaks rotation symmetry in the normal state. This should be contrasted with the scenario considered in Ref. 40, where the anisotropy of the superconducting state originates from nematic orbital order that onsets at high temperature in the normal metal. Furthermore, the nematic superconducting state studied in Ref. 40 is fully gapped and breaks time-reversal state, while the p - or d -wave nematic superconductor studied in our work is time-reversal-symmetric and has point nodes in the gap structure. This can be directly probed in future experiments, including thermal transport and tunneling spectroscopy.

II. CDW MODES COUPLED TO SC

To understand the essential physics of strong density wave fluctuations coupled to SC, we begin by considering a phenomenological GL theory. In GL theory the free energy F_{SC} of the superconductor is expanded up to fourth order in the two-component (spin-singlet) d -wave order parameter $\hat{\Delta} = \Delta \cdot (d_1, d_2)$, i.e., $F_{\text{SC}} = F_{\text{SC}}^{(2)} + F_{\text{SC}}^{(4)}$, with $F_{\text{SC}}^{(4)}$ for the hexagonal systems given by

$$F_{\text{SC}}^{(4)} = \alpha_1 \Delta^4 (|d_1|^2 + |d_2|^2)^2 + \alpha_2 \Delta^4 |d_1^2 + d_2^2|^2, \quad (1)$$

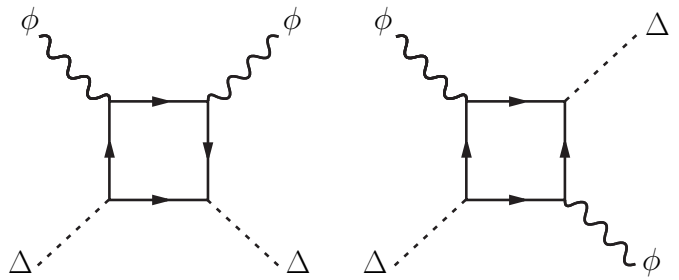


FIG. 1. Two lowest-order diagrams describing coupling between CDW fluctuations ϕ_i and SC order parameter Δ , see Eq. (3). These diagrams are sufficient provided the system is close to the superconducting transition (Δ is small) and the CDW fluctuations are massive.

where $\alpha_{1,2}$ are the GL expansion coefficients. The sign of α_2 determines the SC state below T_c : If $\alpha_2 > 0$, chiral superconducting state has lower energy, $(d_1, d_2) \sim (1, \pm i)$. This state breaks time-reversal symmetry, since $d_i \rightarrow d_i^*$ under time reversal, and is characterized by full pairing gap on the entire Fermi surface. In contrast, if $\alpha_2 < 0$, the order parameter is real and given by $(d_1, d_2) \sim (\cos \theta, \sin \theta)$. This state defines a nematic superconductor, owing its name to the nonzero subsidiary nematic order

$$(N_1, N_2) = (|d_1|^2 - |d_2|^2, d_1^* d_2 + d_1 d_2^*), \quad (2)$$

which transforms as a nematic director; this state has nodes in the excitation spectrum. As shown below, calculating $\alpha_{1,2}$ within weak-coupling gives $\alpha_2 > 0$, selecting the chiral state.

Next, we introduce the coupling to density wave fluctuations. For the sake of definiteness, we consider CDW fluctuations, but note that the argument is similar for SDW fluctuations. In hexagonal systems CDW order is described by a three-component complex order parameter $\phi = (\phi_1, \phi_2, \phi_3)$, where the fields ϕ_i correspond to CDW modes at ordering wave vectors \mathbf{Q}_i . These three wave vectors are related by sixfold rotation. To the lowest order, the coupling of the SC order parameter \mathbf{d} to the CDW modes ϕ , shown diagrammatically in Fig. 1, can be expressed as

$$F_{\phi-\Delta} = \beta_1 |\phi|^2 |\mathbf{d}|^2 + \beta_2 (P_1 N_1 + P_2 N_2). \quad (3)$$

Here $(P_1, P_2) = (2|\phi_1|^2 - |\phi_2|^2 - |\phi_3|^2, \sqrt{3}(|\phi_2|^2 - |\phi_3|^2))$ is a subsidiary nematic order parameter quadratic in the fields ϕ_i and describes anisotropic CDW fluctuations which transform as partners under rotations, and $\mathbf{d} = (d_1, d_2)$. Since it has the same symmetry as (N_1, N_2) in (2) it couples linearly.

We further assume that the fields ϕ_i are massive and can be described by a Gaussian contribution F_ϕ , the precise form of which is immaterial for present purpose. The free energy of the superconductor coupled to the CDW fluctuations can thus be expressed as $F =$

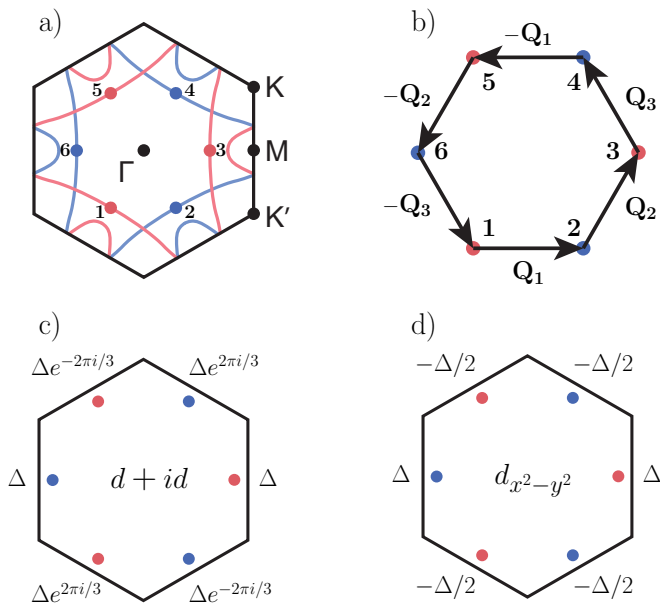


FIG. 2. (a) Fermi surface of twisted bilayer graphene slightly away from Van Hove singularity. Blue and red parts originate from different valleys. (b) Hot spots are connected by six inequivalent CDW/SDW wavevectors $\pm \mathbf{Q}_i$, related by six-fold rotations. For concreteness, we assume that $\pm \mathbf{Q}_i$ connect adjacent hot spots. (c) Time-reversal-breaking chiral superconductivity is realized if $\alpha_2 > 0$, see Eq. (1), while (d) the rotational symmetry-breaking nematic state has lower energy provided $\alpha_2 < 0$.

$F_\Delta + F_\phi + F_{\psi-\Delta}$. Since the fields ϕ_i are massive they can be integrated out, which leads to an effective free energy for the superconductor given by $F_{\text{SC}} = F_\Delta + \delta F_\Delta$; at fourth order, the correction $\delta F_\Delta^{(4)}$ is given by

$$\delta F_\Delta^{(4)} \sim -\beta_1^2 |\mathbf{d}|^4 - 2\beta_2^2 (N_1^2 + N_2^2). \quad (4)$$

Using the identity $N_1^2 + N_2^2 = |d_1^2 + d_2^2|^2$, we observe that (4) implies a lowering of the energy of the nematic superconducting state relative to the chiral state. This effect is enhanced as the fluctuations become stronger, thus exceeding the weak-coupling or any other fourth-order contribution and eventually leading to NSC. Remarkably, the argument leading to Eq. (4) is general and does not rely on the nature of the fluctuating field. In particular, as mentioned, it also applies to SDW fluctuations, which can be described by a vectorial order parameter $\vec{\phi} = (\vec{\phi}_1, \vec{\phi}_2, \vec{\phi}_3)$. Finally, a similar argument was applied to demonstrate the existence of $s + d$ -wave SC state in the presence of nematic fluctuations in systems with tetragonal symmetry⁶³.

III. GENERAL MODEL FOR CDW FLUCTUATIONS AND SC

While the above argument is physically compelling and correctly captures the physical mechanism of fluctuation-

induced NSC, it is based on a simplified approach which neglects the contribution of modes with nonzero momentum or frequency. To develop a theory of NSC which takes this into account, we now consider a more general model for a two-component d -wave superconductor in the presence of CDW fluctuations. The Hamiltonian of such a system is given by $H = H_\psi + H_\phi + H_{\psi-\Delta} + H_{\psi-\phi}$, where

$$H_\psi = \sum_{\mathbf{k}\alpha} \xi_{\mathbf{k}} \psi_{\mathbf{k}\alpha}^\dagger \psi_{\mathbf{k}\alpha}, \quad H_\phi = \frac{1}{2} \sum_{\mathbf{q}} \tilde{V}_0^{-1}(\mathbf{q}) \phi_{\mathbf{q}} \phi_{-\mathbf{q}} \quad (5)$$

describe the normal state electronic excitations $\psi_{\mathbf{k}\alpha}$ with dispersion $\xi_{\mathbf{k}}$ and spin $\alpha = \uparrow, \downarrow$, and the (bosonic) CDW fluctuations $\phi_{\mathbf{q}}$ governed by the bare propagator $\tilde{V}_0(\mathbf{q})$, respectively. The propagator $\tilde{V}_0(\mathbf{q})$ is peaked at the six symmetry-related CDW ordering vectors $\pm \mathbf{Q}_{i=1,2,3}$. The coupling of the fermions to the superconducting pair potential and the CDW fluctuations is given by

$$H_{\psi-\Delta} = \frac{1}{2} \sum_{\mathbf{k}} \left(\psi_{\mathbf{k}\uparrow}^\dagger \psi_{-\mathbf{k}\downarrow}^\dagger - \psi_{\mathbf{k}\downarrow}^\dagger \psi_{-\mathbf{k}\uparrow}^\dagger \right) \Delta_{\mathbf{k}} + \text{H.c.},$$

$$H_{\psi-\phi} = \lambda \sum_{\mathbf{k}, \mathbf{q}} \psi_{\mathbf{k}+\mathbf{q}\alpha}^\dagger \psi_{\mathbf{k}\alpha} \phi_{\mathbf{q}}, \quad (6)$$

respectively. On the Fermi surface, the pairing potential of the two-component d -wave SC is given by $\Delta_{\mathbf{k}} = \Delta [2d_1 \hat{k}_x \hat{k}_y + d_2 (\hat{k}_x^2 - \hat{k}_y^2)]$, where, again, Δ is the overall pairing strength and $\mathbf{d} = (d_1, d_2)$, which satisfies $|\mathbf{d}|^2 = 1$, captures the structure of the two-component order parameter. This form of the pairing potential corresponds to the E_2 representation of the point group D_6 .

The Hamiltonian H of Eqs. (5) and (6) defines a general model for a d -wave superconductor coupled to CDW fluctuations. To demonstrate how the (gapped) fluctuations can induce NSC via the so-called feedback mechanism, we proceed in two main steps: First, we integrate out the fermions and then the fluctuation fields $\phi_{\mathbf{q}}$. In this way, we obtain an effective free energy functional for the superconducting order parameter which includes the effect of CDW fluctuations and renormalizes the weak-coupling result. The latter is directly obtained from H by neglecting the effect of CDW fluctuations altogether. More precisely, within weak-coupling the BCS free energy of the superconductor is given by $F_\Delta = -T \ln [\text{Tr} \exp(-H_0/T)]$, where $H_0 = H_\psi + H_{\psi-\Delta}$. After straightforward evaluation, we find F_Δ in hexagonal systems up to fourth order as (see Appendix A for details)

$$F_\Delta = r\Delta^2 |\mathbf{d}|^2 + K_0 \Delta^4 (2|\mathbf{d}|^4 + |\mathbf{d}^2|^2), \quad (7)$$

where $r \sim (T - T_c)$, $K_0 = (T/16) \sum_{\omega_n, \mathbf{k}} (\omega_n^2 + \xi_{\mathbf{k}}^2)^{-2}$, and $\omega_n = \pi T(2n + 1)$ are fermionic Matsubara frequencies. Since $K_0 > 0$, we find that within weak-coupling the chiral state indeed has lower energy below T_c , in agreement

with Ref. 29. This applies very generally to systems with hexagonal symmetry and does not depend on microscopic details of Fermi surface.

IV. FLUCTUATION-INDUCED NSC

We now proceed to calculate the correction to the weak-coupling free energy originating from the CDW fluctuations. As an intermediate step, we consider the normal state electronic structure described by $\xi_{\mathbf{k}}$ of (5) in more detail. At low energies, the most important electronic excitations are located in the vicinity of those points on the Fermi surface which are connected by the CDW ordering vectors, the so-called hot spots. The hexagonal symmetry dictates that there are six such hot spots. Following the results of Ref. 36, we focus on CDWs with wavevectors that connect all adjacent hot spots, as shown in Fig. 2(b), though this assumption is not important for our analysis. This hot spot model, which introduces six flavors of low-energy fermions $\psi_{i\mathbf{k}\alpha}$ ($i = 1, \dots, 6$) with corresponding $\xi_{i\mathbf{k}}$, also establishes a natural connection with TBG^{36,41}. Note that within the hot spot model all momenta are measured with respect to the hot spots.

To calculate the feedback correction, we integrate out the CDW fluctuations, which we assume to be massive, and determine their contribution to the free energy. Importantly, this contribution depends on the SC order parameter and can be expanded in Δ to obtain renormalized GL coefficients. Since the full calculation is tedious but straightforward, we discuss only the final result and present the details in Appendix A. We find the correction to the free energy due to CDW fluctuations as

$$\delta F_{\Delta} = -T \text{Tr}(\hat{V}\delta\hat{\chi}) - \frac{T}{2} \text{Tr}(\hat{V}\delta\hat{\chi})^2 + \dots, \quad (8)$$

where \hat{V} is an effective propagator of the CDW fluctuations, and $\delta\hat{\chi}$ is the correction to the CDW susceptibility due to the coupling to Δ . Note that in (8) Tr implies summation over frequencies, momenta, as well as patches. Near T_c , $\delta\hat{\chi}$ can be expanded in powers of Δ , with the lowest-order term proportional to Δ^2 . This term is diagrammatically shown in Fig. 1 and in the limit of zero frequency and momentum has exactly the form of Eq. (3). As a result, the term in Eq. (8) proportional to $\text{Tr}(\hat{V}\delta\hat{\chi})^2$ gives rise to a quartic correction $\delta F_{\Delta}^{(4)}$ to the free energy of the superconductor and shifts the energetic balance towards the nematic state, in agreement with Eq. (4). As we discuss in Appendix A, the effect of the term proportional to $\text{Tr}(\hat{V}\delta\hat{\chi})$ is less important and can be neglected as the strength of fluctuations increases.

Remarkably, we find that δF_{Δ} always favors nematic SC, irrespective of the precise form of $\hat{V}(\Omega, \mathbf{q})$ or $\xi_{\mathbf{k}}$, provided CDW fluctuations are sufficiently strong. This result solely relies on the form of $\delta\hat{\chi}$, and is a direct generalization of Eq. (4) for the case when CDW modes with

nonzero Ω and q are taken into account. Specifically, for the model described by Eqs. (5) and (6), the leading contribution to the fourth-order free energy feedback correction $\delta F_{\Delta}^{(4)}$ reads as

$$\delta F_{\Delta}^{(4)} = -\frac{3T^3(\lambda\Delta)^4}{2} [(Y_1 + 8Y_2 + 8Y_3 + 8Y_4)|\mathbf{d}|^4 + 2(Y_1 + 2Y_2 + 2Y_3 - Y_4)|\mathbf{d}^2|^2], \quad (9)$$

with

$$Y_1 \equiv \sum_{\mathbf{q}, \Omega_m} V^2(\mathbf{q})K_2^2(\mathbf{q}), \quad Y_3 \equiv \sum_{\mathbf{q}, \Omega_m} V^2(\mathbf{q})K_1(\mathbf{q})K_2(\mathbf{q}), \\ Y_2 \equiv \sum_{\mathbf{q}, \Omega_m} V^2(\mathbf{q})K_1^2(\mathbf{q}), \quad Y_4 \equiv \sum_{\mathbf{q}, \Omega_m} V^2(\mathbf{q})K_1(\mathbf{q})K_1(-M\mathbf{q}), \quad (10)$$

and the functions K_1 and K_2 are defined as

$$K_1(\mathbf{q}, \Omega_m) \equiv \sum_{\mathbf{k}, \omega_n} \frac{\omega_n(\omega_n + \Omega_m) - \xi_{1\mathbf{k}}\xi_{2\mathbf{k}-\mathbf{q}}}{[\omega_n^2 + \xi_{1\mathbf{k}}^2]^2 [(\omega_n + \Omega_m)^2 + \xi_{2\mathbf{k}-\mathbf{q}}^2]}, \\ K_2(\mathbf{q}, \Omega_m) \equiv \sum_{\mathbf{k}, \omega_n} \frac{1}{[\omega_n^2 + \xi_{1\mathbf{k}}^2] [(\omega_n + \Omega_m)^2 + \xi_{2\mathbf{k}-\mathbf{q}}^2]}. \quad (11)$$

Here $\xi_{1,2\mathbf{k}}$ are the dispersions of the hot spot fermions, see Fig. 2, which are related by the mirror symmetry M as $\xi_{2\mathbf{k}} = \xi_{1M\mathbf{k}}$. $\omega_n = \pi T(2n + 1)$ and $\Omega_m = 2\pi Tm$ are fermionic and bosonic Matsubara frequencies, respectively, and we have suppressed Ω_m in (10) for brevity. Since $V(\Omega, \mathbf{q})$ in (10) is the CDW propagator within the hot spot model it is peaked at $\mathbf{q} = 0$; $V(\Omega, \mathbf{q})$ is related to the (effective) propagator of the full model \tilde{V} as $V(\Omega, \mathbf{q}) \equiv \tilde{V}(\Omega, \mathbf{Q}_1 + \mathbf{q})$, where \mathbf{Q}_1 connects hot spots 1 and 2, see Fig. 2.

Our claim that the feedback effect of CDW fluctuations always favors NSC now follows from Eq. (9): It is easily demonstrated that the coefficient of $|d_1^2 + d_2^2|^2$ is always positive, i.e., $Y_1 + 2Y_2 + 2Y_3 - Y_4 > 0$, thus proving our statement. Importantly, Eq. (9) does not require any assumptions about the explicit form of $V(\Omega, \mathbf{q})$ or $\xi_{i\mathbf{k}}$, and only relies on the (rotation and mirror) symmetries relating the hot spots. Furthermore, when $V(\Omega, q)$ is strongly peaked at $\Omega = q = 0$, we exactly recover Eqs. (3)-(4) with

$$\beta_1 = T(\lambda T\Delta)^2 [4K_1(0, 0) + K_2(0, 0)], \\ \beta_2 = T(\lambda T\Delta)^2 [K_1(0, 0) + K_2(0, 0)]. \quad (12)$$

The overall prefactor in Eq. (4) is proportional to $\sum_{\mathbf{q}} V^2(0, q)$, implying that the feedback contribution becomes more significant as the strength of CDW fluctuations grows. As such, Eq. (9) in combination with (4) represents the central result of this paper.

Finally, we consider a specific model for twisted bilayer graphene to exemplify our results. We assume that

the effective normal-state CDW propagator is given by $V(q) = \chi_0/c^2(q_0^2 + q^2)$. We use the Fermi surface reproduced from the band structure calculation for TBG with filling factor close to the filling of two electrons/holes per supercell⁶⁴, see Fig. 2(a). The dispersion near the hot spots can be approximated as $\xi_{i\mathbf{k}} = v(\mathbf{k} \cdot \mathbf{n}_i)$, where \mathbf{n}_i is the unit vector in the direction ΓM_i . The feedback correction to free energy then equals

$$\delta F_{\Delta}^{(4)} = -\frac{13.46}{(2\pi)^4} \left(\frac{\chi_0 T \lambda^2}{q_0 v^2 c^2} \right)^2 \frac{\Delta^4}{T^3} (1.16|\mathbf{d}|^4 + |\mathbf{d}^2|^2). \quad (13)$$

As the strength of the fluctuations increases, i.e., as q_0 becomes smaller, this correction becomes more significant, eventually exceeding the weak-coupling contribution and leading to NSC. We emphasize that while the numerical prefactors in (13) depend on the particular model chosen, the results given by Eqs. (9)–(11) were derived without specifying the normal-state dispersion $\xi_{i\mathbf{k}}$ and normal-state CDW propagator $V(\Omega, \mathbf{q})$, and thus apply very generally. In particular, it can be used in the case when the Fermi energy is close to Van Hove singularity, and the hot spot dispersion (in proper coordinates) is given by $\xi_{\mathbf{k}} = Ak_x^2 - Bk_y^2$ with some constants $A, B > 0$. In the latter case, we reach the same qualitative conclusion that sufficiently strong density wave fluctuations stabilize NSC (see Appendix A 6 for details).

The analysis for the case of strong SDW fluctuations in a d -wave superconductor is similar. The important difference, however, is the relative minus sign between two diagrams in Fig. 1. This leads to the destructive interference for the coherence factor in the expression for $\delta\hat{\chi}$ ⁶⁵. It is straightforward to show that all results for SDW fluctuations, apart from a possible overall numerical prefactor, can be obtained from the CDW case simply by changing $K_2(\mathbf{q}, \Omega) \rightarrow -K_2(\mathbf{q}, \Omega)$, which leads to the partial (but not complete) suppression of the feedback contribution to free energy (see Appendix B).

V. CONCLUSION

In conclusion, by going beyond weak-coupling and including fluctuations of a density wave order we have presented a general mechanism for nematic multicomponent superconductivity in 2D. The theory we develop can be directly applied to twisted bilayer graphene, where density wave fluctuations are strong due to Fermi surface nesting and intertwined with d/p -wave superconductivity³⁶. Together with the recent observation of the upper critical magnetic field anisotropy in

twisted bilayer graphene², this serves as a main experimental motivation for our work.

As mentioned in the introduction, in our theory the onset of nematicity is tied to pairing. Since nematicity appears as the composite order parameter of Eq. (2), we expect that the two transitions can be separated, i.e., the nematic transition can occur at a higher temperature than the superconducting transition, giving rise to a vestigial nonsuperconducting phase with broken rotation symmetry^{23,55,66}. To assess the possibility of a vestigial nematic phase one must go beyond the theory developed here and consider the fluctuations of superconducting order parameter. We leave this as a direction for the future.

Finally, we notice that, alternatively to the strongly-correlated scenario considered in this paper, NSC may, in principle, originate from the internal strain. Indeed, symmetry allows the coupling between the nematic subsidiary order (2) and the components of the strain tensor u_{ij} of the form²⁰

$$F_{\text{strain}} = g[(u_{xx}^2 - u_{yy}^2)N_1 + 2u_{xy}N_2]. \quad (14)$$

It is clear from this expression that in the presence of uniaxial strain, $u_{xx}^2 - u_{yy}^2 \neq 0$, one of the superconducting components develops order at higher temperature than the other one, thus resulting in nematic superconductivity. If strain is not too strong, the effect of nematicity becomes weaker as one lowers the temperature²⁰, and eventually NSC transits into a chiral superconductor at sufficiently small temperature. To distinguish between the scenarios for NSC from density wave fluctuations and from internal strain, as well as from the strain-induced nematicity in s -wave superconductor, a detailed study of the upper critical field behavior in different regimes is required.

VI. ACKNOWLEDGMENTS

We greatly acknowledge the discussions with Pablo Jarillo-Herrero, Yuan Cao, Daniel Rodan-Legrain, and Oriol Rubies-Bigorda, who shared with us their unpublished experimental data. We also thank Rafael Fernandes, Jonathan Ruhman, and Max Metlitski for numerous valuable discussions. This work is supported by DOE Office of Basic Energy Sciences, Division of Materials Sciences and Engineering under Award DE-SC0018945. LF is partly supported by the David and Lucile Packard Foundation. J.W.F.V. was supported by the National Science Foundation MRSEC Program, under Grant No. DMR-1720530.

Appendix A: Nematic d -wave superconductivity in presence of charge density wave fluctuations

In this appendix, we present a detailed calculation of the feedback correction to the free energy of a two-component superconductor due to the presence of charge density wave (CDW) fluctuations. For definiteness, we focus on a d -wave superconductor. First, we derive the effective imaginary time action that describes the interplay between pairing potential and the density wave fluctuations. Next, we calculate the very general expression for the feedback contribution to free energy. Finally, we apply our results to particular models which are relevant to twisted bilayer graphene.

1. The model description and the effective action

As was discussed in the main text, the presence of density wave fluctuations allows us to focus on the vicinities of the points on the Fermi surface connected by the density wave ordering wave vectors, so-called hot spots. The corresponding regions in momentum space near hot spots are called patches. We consider a 2D model with six nonequivalent hot spots in the Brillouin zone, with the CDW wavevectors connecting adjacent hot spots, see Fig. 3. Then, Hamiltonian (5)-(6) of the main text in the low-energy limit translates into the imaginary time action for six patches

$$S = S_\psi + S_\phi + S_{\psi-\Delta} + S_{\psi-\phi}. \quad (\text{A1})$$

The first term describes the noninteracting electrons near hot spots:

$$S_\psi = T \sum_{i=1}^6 \sum_{\omega_n, \mathbf{k}} (-i\omega_n + \xi_{i\mathbf{k}}) \psi_{i\alpha}^\dagger(\omega_n, \mathbf{k}) \psi_{i\alpha}(\omega_n, \mathbf{k}). \quad (\text{A2})$$

Here, $\omega_n = 2\pi T(n + 1/2)$ are fermionic Matsubara frequencies, index $i = 1, \dots, 6$ numerates hot spots, $\xi_i(\mathbf{k})$ is a dispersion near the i -th hot spot, and the summation over repeated spin indices $\alpha = \uparrow, \downarrow$ is implied. We assume the presence of sixfold rotational symmetry in the system, which implies that the dispersions near adjacent hot spots are related as $\xi_i(\mathbf{k}) = \xi_{i+1}(R_6\mathbf{k})$, where $R_6 = \{\{1/2, -\sqrt{3}/2\}, \{\sqrt{3}/2, 1/2\}\}$ is the $\pi/3$ rotation matrix. This results in an additional relation that we will actively use, $\xi_i(-\mathbf{k}) = \xi_{i+3}(\mathbf{k})$, where the hot spot index i is defined mod 6. Finally, we assume that different hot spots with indices i and j are related by a mirror symmetry M_{ij} , which leads to another useful equality $\xi_i(\mathbf{k}) = \xi_j(M_{ij}\mathbf{k})$.

The second term in Eq. (A1) is a quadratic action for CDW fluctuations:

$$S_\phi = \frac{T}{2} \sum_{i=1}^6 \sum_{\Omega_m, \mathbf{q}} V_{0i}^{-1}(\mathbf{q}) \phi_i(\Omega_m, \mathbf{q}) \phi_i^*(\Omega_m, \mathbf{q}), \quad (\text{A3})$$

where $\Omega_m = 2\pi Tm$ are bosonic Matsubara frequencies and index $i = 1, \dots, 6$ numerates CDW fluctuations with different ordering wavevectors. The fields $\phi_i(\mathbf{q})$ should be viewed as 'shifted' with respect to the global CDW field $\phi(\mathbf{q})$ introduced in Eqs. (5)-(6) of the main text, i.e., $\phi_i(\mathbf{q}) \equiv \phi(\mathbf{Q}_i + \mathbf{q})$, where CDW wavevectors \mathbf{Q}_i connect hot spots with indices i and $i+1$ as shown in Fig. 3(a). We assume that the relevant bosonic momenta are much smaller than the distance between the hot spots, $q \ll Q$. Even though the propagator for the global field $\phi(\mathbf{q})$, $\tilde{V}_0(\mathbf{q})$, is peaked at \mathbf{Q}_i , the propagators of fields $\phi_i(\mathbf{q})$ are apparently peaked at $\mathbf{q} = 0$, so $V_{0i}(\mathbf{q})$ can be thought of as, e.g., Lorentzians with the maximum at $q = 0$. The particular form of $V_{0i}(\mathbf{q})$, however, is not important for us at this moment. Finally, since the global field $\phi(\mathbf{r})$ is real, the different 'shifted' components $\phi_i(\Omega, \mathbf{q})$ are not independent, but related according to $\phi_{i+3}(-\Omega, -\mathbf{q}) = [\phi_i(\Omega, \mathbf{q})]^*$.

The third term in Eq. (A1) describes the two-component d -wave pairing,

$$S_{\psi-\Delta} = \frac{T}{2} \sum_{\omega_n, \mathbf{k}} \tilde{\Delta}_{ij} \varepsilon_{\alpha\beta} \psi_{i\alpha}^\dagger(\omega_n, \mathbf{k}) \psi_{j\beta}^\dagger(-\omega_n, -\mathbf{k}) + \text{H. c.}, \quad (\text{A4})$$

where $\varepsilon_{\alpha\beta}$ is the Levi-Civita tensor in spin space, and the pairing matrix $\tilde{\Delta}$ is given by

$$\tilde{\Delta} = \Delta \cdot I_{\text{spin}} \otimes \left[\frac{\sqrt{3}}{2} d_1 \begin{pmatrix} 0 & 0 & 0 & 1 & 0 & 0 \\ 0 & 0 & 0 & 0 & -1 & 0 \\ 0 & 0 & 0 & 0 & 0 & 0 \\ 1 & 0 & 0 & 0 & 0 & 0 \\ 0 & -1 & 0 & 0 & 0 & 0 \\ 0 & 0 & 0 & 0 & 0 & 0 \end{pmatrix} + d_2 \begin{pmatrix} 0 & 0 & 0 & -1/2 & 0 & 0 \\ 0 & 0 & 0 & 0 & -1/2 & 0 \\ 0 & 0 & 0 & 0 & 0 & 1 \\ -1/2 & 0 & 0 & 0 & 0 & 0 \\ 0 & -1/2 & 0 & 0 & 0 & 0 \\ 0 & 0 & 1 & 0 & 0 & 0 \end{pmatrix} \right]_{\text{patches}}. \quad (\text{A5})$$

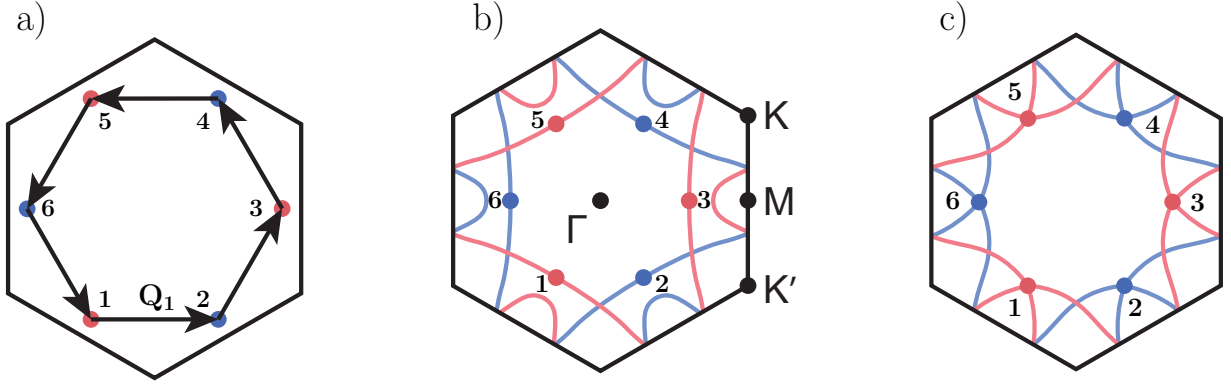


FIG. 3. (a) Six inequivalent hot spots in the Brillouin zone are connected by CDW wavevectors \mathbf{Q}_i . All \mathbf{Q}_i connect hot spots with numbers i and $i + 1$, and can be obtained from \mathbf{Q}_1 by sixfold rotations. (b) Fermi surface in twisted bilayer graphene above the Van Hove singularity. (c) Fermi surface of twisted bilayer graphene at Van Hove energy. This scenario is realized when the filling factor is close to $n = 2$ electrons/holes per supercell. Blue and red parts of the Fermi surface originate from different valleys.

Here (d_1, d_2) plays the role of a two-component superconducting order parameter, and, again, summation over repeated spin indices $\alpha, \beta = \uparrow, \downarrow$ and patch indices $i, j = 1, \dots, 6$ is implied.

Finally, the coupling between electrons and CDW fluctuations is described by the last term in Eq. (A1):

$$\begin{aligned}
 S_{\psi-\phi} &= \lambda T^2 \sum_{i=1}^6 \sum_{\omega_n, \Omega_m} \sum_{\mathbf{k}, \mathbf{q}} \psi_{i+1\alpha}^\dagger(\omega_n + \Omega_m, \mathbf{k} + \mathbf{q}) \psi_{i\alpha}(\omega_n, \mathbf{k}) \phi_i(\Omega_m, \mathbf{q}) + \text{H. c.} = \\
 &= T \sum_{i,j=1}^6 \sum_{\omega_n, \Omega_m} \sum_{\mathbf{k}, \mathbf{q}} \psi_{i\alpha}^\dagger(\omega_n + \Omega_m, \mathbf{k} + \mathbf{q}) \psi_{j\alpha}(\omega_n, \mathbf{k}) \hat{\Sigma}_{ij}(\Omega_m, \mathbf{q}), \tag{A6}
 \end{aligned}$$

with $\hat{\Sigma}(\mathbf{q}, \Omega)$ defined as

$$\hat{\Sigma}(\Omega, \mathbf{q}) = \lambda T \cdot I_{\text{spin}} \otimes \begin{pmatrix} 0 & \phi_4(\Omega, \mathbf{q}) & 0 & 0 & 0 & \phi_6(\Omega, \mathbf{q}) \\ \phi_1(\Omega, \mathbf{q}) & 0 & \phi_5(\Omega, \mathbf{q}) & 0 & 0 & 0 \\ 0 & \phi_2(\Omega, \mathbf{q}) & 0 & \phi_6(\Omega, \mathbf{q}) & 0 & 0 \\ 0 & 0 & \phi_3(\Omega, \mathbf{q}) & 0 & \phi_1(\Omega, \mathbf{q}) & 0 \\ 0 & 0 & 0 & \phi_4(\Omega, \mathbf{q}) & 0 & \phi_2(\Omega, \mathbf{q}) \\ \phi_3(\Omega, \mathbf{q}) & 0 & 0 & 0 & \phi_5(\Omega, \mathbf{q}) & 0 \end{pmatrix}_{\text{patches}}. \tag{A7}$$

To proceed, we introduce Nambu particle-hole space according to

$$\Psi_i(\omega, \mathbf{k}) = \begin{pmatrix} \psi_{i\uparrow}(\omega, \mathbf{k}) \\ \psi_{i\downarrow}(\omega, \mathbf{k}) \\ \psi_{i+3\downarrow}^\dagger(-\omega, -\mathbf{k}) \\ -\psi_{i+3\uparrow}^\dagger(-\omega, -\mathbf{k}) \end{pmatrix}_N. \tag{A8}$$

Then, using the identity $\xi_i(-\mathbf{k}) = \xi_{i+3}(\mathbf{k})$, the action (A1) can be conveniently rewritten as

$$\begin{aligned}
 S_\psi &= -\frac{T}{2} \sum_{i=1}^6 \sum_{\omega_n, \mathbf{k}} \Psi_{i\alpha}^\dagger(\omega_n, \mathbf{k}) G_{0i}^{-1}(\omega_n, \mathbf{k}) \Psi_{i\alpha}(\omega_n, \mathbf{k}), \\
 S_{\psi-\Delta} &= \frac{T}{2} \sum_{\omega_n, \mathbf{k}} \Psi^\dagger(\omega_n, \mathbf{k}) \Sigma_\Delta \Psi(\omega_n, \mathbf{k}), \\
 S_{\psi-\phi} &= \frac{T}{2} \sum_{\omega_n, \Omega_m} \sum_{\mathbf{k}, \mathbf{q}} \Psi^\dagger(\omega_n + \Omega_m, \mathbf{k} + \mathbf{q}) \Sigma_\phi(\Omega_m, \mathbf{q}) \Psi(\omega_n, \mathbf{k}), \tag{A9}
 \end{aligned}$$

with

$$G_{0i}(\omega, \mathbf{k}) = -\frac{i\omega + \xi_{i\mathbf{k}}\tau_z}{\omega^2 + \xi_{i\mathbf{k}}^2} \otimes I_{\text{spin}}, \quad \Sigma_\Delta = \begin{pmatrix} 0 & \hat{\Delta} \\ \hat{\Delta}^\dagger & 0 \end{pmatrix}_N, \quad \Sigma_\phi(\Omega, \mathbf{q}) = \hat{\Sigma}(\Omega, \mathbf{q}) \otimes \tau_z. \quad (\text{A10})$$

Here, $\hat{\Sigma}$ is given by Eq. (A7), τ_i are Pauli matrices in Nambu space, and $\hat{\Delta}$ equals

$$\hat{\Delta} = \Delta \cdot I_{\text{spin}} \otimes \left[\frac{\sqrt{3}}{2} d_1 \begin{pmatrix} 1 & 0 & 0 & 0 & 0 & 0 \\ 0 & -1 & 0 & 0 & 0 & 0 \\ 0 & 0 & 0 & 0 & 0 & 0 \\ 0 & 0 & 0 & 1 & 0 & 0 \\ 0 & 0 & 0 & 0 & -1 & 0 \\ 0 & 0 & 0 & 0 & 0 & 0 \end{pmatrix} + d_2 \begin{pmatrix} -1/2 & 0 & 0 & 0 & 0 & 0 \\ 0 & -1/2 & 0 & 0 & 0 & 0 \\ 0 & 0 & 1 & 0 & 0 & 0 \\ 0 & 0 & 0 & -1/2 & 0 & 0 \\ 0 & 0 & 0 & 0 & -1/2 & 0 \\ 0 & 0 & 0 & 0 & 0 & 1 \end{pmatrix} \right]_{\text{patches}}. \quad (\text{A11})$$

We note that $\hat{\Delta}$ has matrix structure different from $\tilde{\Delta}$, Eq. (A5), because Nambu space introduced in Eq. (A8) mixes different patch indices.

Combining Eqs. (A3) and (A9), action (A1) takes simple form

$$S = S_\phi + \frac{T}{2} \text{Tr} \Psi^\dagger (-G_0^{-1} + \Sigma_\Delta + \Sigma_\phi) \Psi, \quad (\text{A12})$$

where $G_0 = \text{diag}\{G_{0i}\}_{\text{patches}}$, and Tr implies trace over spin, Nambu, and patch indices, as well as summation over momenta and frequencies.

To derive the effective theory that describes interplay between CDW fluctuations ϕ_i and SC order parameter d_i , we integrate out fermions:

$$\begin{aligned} & \int D\psi^\dagger D\psi \exp \left[-\frac{T}{2} \Psi^\dagger (-G_0^{-1} + \Sigma_\Delta + \Sigma_\phi) \Psi \right] = \{ \text{Det} [T (-G_0^{-1} + \Sigma_\Delta + \Sigma_\phi)] \}^{1/2} = \\ & = \exp \left\{ \frac{1}{2} \text{Tr} \ln [T (-G_0^{-1} + \Sigma_\Delta + \Sigma_\phi)] \right\} = [\text{Det} (-TG_0^{-1})]^{1/2} \exp \left[\frac{1}{2} \text{Tr} \ln (1 - G_0 \Sigma_\Delta - G_0 \Sigma_\phi) \right]. \end{aligned} \quad (\text{A13})$$

Neglecting the normal-state electronic part of the partition function, $[\text{Det} (-TG_0^{-1})]^{1/2}$ (which does not depend on ϕ or Δ), we find that CDW fluctuations in the presence of pairing potential are described by the effective partition function Z_{eff} given by

$$Z_{\text{eff}} = \int D\phi \exp \left[-S_\phi + \frac{1}{2} \text{Tr} \ln (1 - G_0 \Sigma_\Delta - G_0 \Sigma_\phi) \right]. \quad (\text{A14})$$

From this expression, we can extract the effective action:

$$S_{\text{eff}} = S_\phi - \frac{1}{2} \text{Tr} \ln (1 - G_0 \Sigma_\Delta - G_0 \Sigma_\phi). \quad (\text{A15})$$

All transformations so far have been exact. Now we make some assumptions that allow us to proceed with our calculation. First, we consider the vicinity of the superconducting transition temperature T_c , so we expand the effective action in powers of small pairing potential Δ (equivalently, in powers of Σ_Δ) up to fourth order. Second, we assume that CDW fluctuations, though strong, remain massive. Hence, we expand the effective action up to second order in ϕ (equivalently, in Σ_ϕ).

Expanding the logarithm in Eq. (A15), we find

$$\begin{aligned} S_{\text{eff}} & \approx S_\Delta + S_\phi + \delta S_\phi + S_{\phi-\Delta}, \\ \delta S_\phi & = \frac{1}{4} \text{Tr} (G_0 \Sigma_\phi)^2, \quad S_\Delta = \frac{1}{4} \text{Tr} (G_0 \Sigma_\Delta)^2 + \frac{1}{8} \text{Tr} (G_0 \Sigma_\Delta)^4, \\ S_{\phi-\Delta} & = \frac{1}{2} \text{Tr} [(G_0 \Sigma_\Delta)^2 (G_0 \Sigma_\phi)^2] + \frac{1}{4} \text{Tr} [(G_0 \Sigma_\Delta G_0 \Sigma_\phi)^2] + \\ & + \frac{1}{2} \text{Tr} [(G_0 \Sigma_\phi)^2 (G_0 \Sigma_\Delta)^4] + \frac{1}{2} \text{Tr} [(G_0 \Sigma_\Delta)^2 (G_0 \Sigma_\Delta G_0 \Sigma_\phi)^2] + \frac{1}{4} \text{Tr} [(G_0 \Sigma_\Delta G_0 \Sigma_\Delta G_0 \Sigma_\phi)^2]. \end{aligned} \quad (\text{A16})$$

Here, S_Δ is a weak-coupling part of Ginzburg-Landau free energy of a superconductor. Terms S_ϕ and δS_ϕ are bare bosonic propagator, Eq. (A3), and the normal-state CDW susceptibility, respectively. Finally, $S_{\phi-\Delta}$ describes the interplay between CDW fluctuations and superconductivity, which eventually results in the feedback correction to free energy. The different terms in $S_{\phi-\Delta}$ are shown diagrammatically in Fig. 4 and will be explicitly calculated below.

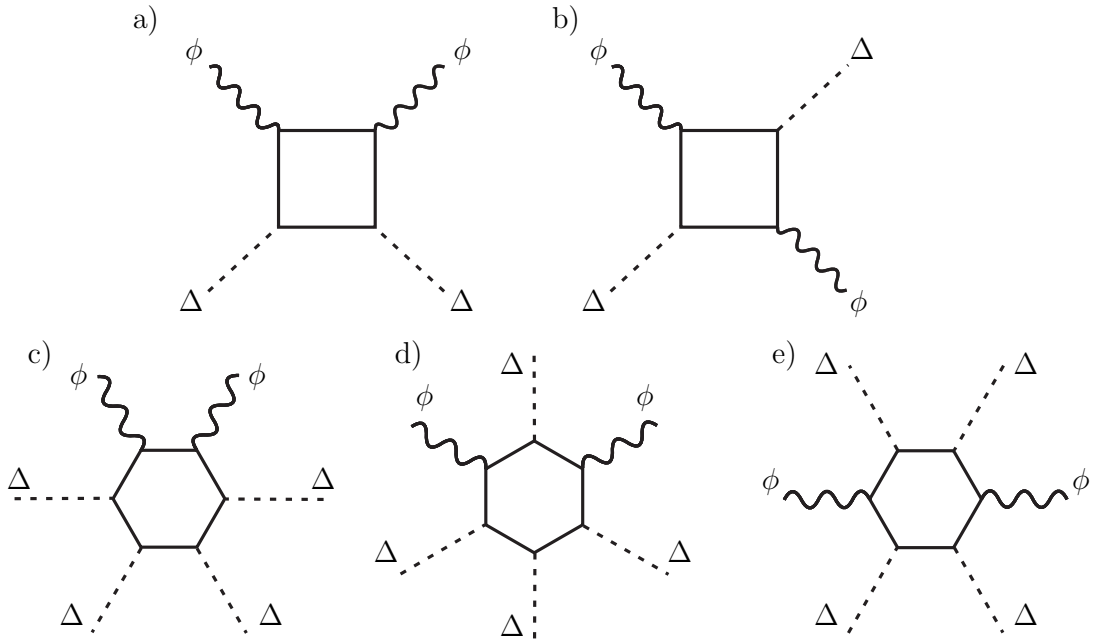


FIG. 4. Diagrams describing the coupling between pairing potential $\Delta(d_1, d_2)$ and density wave fluctuations ϕ_i . Diagrams (a)-(b) schematically represent the coupling $\phi^2 d^2$ and describe the Δ^2 correction to CDW susceptibility, while diagrams (c)-(e) correspond to the coupling $\phi^2 d^4$ contributing the Δ^4 correction to CDW susceptibility. The contribution to the feedback free energy from diagrams (a)-(b) becomes dominant when fluctuations become sufficiently strong.

2. Weak-coupling analysis

In this section, we calculate the fourth-order weak-coupling contribution to free energy. The corresponding part of the effective action is given by

$$S_{\Delta}^{(4)} = \frac{1}{8} \text{Tr}[(G_0 \Sigma_{\Delta})^4] = X_0 \Delta^4 \left[2(|d_1|^2 + |d_2|^2)^2 + |d_1^2 + d_2^2|^2 \right], \quad X_0 = \frac{3}{8} \sum_{\omega_n, \mathbf{k}} \left(\frac{1}{\omega_n^2 + \xi_{i\mathbf{k}}^2} \right)^2 > 0, \quad (\text{A17})$$

where $\xi_{i\mathbf{k}}$ is a dispersion near any of the hot spots, and no summation over i is needed here. The weak-coupling free energy then equals

$$F_{\Delta}^{(4)} = -T \ln Z_{\Delta}^{(4)} = T X_0 \Delta^4 \left[2(|d_1|^2 + |d_2|^2)^2 + |d_1^2 + d_2^2|^2 \right]. \quad (\text{A18})$$

This result is a 'hot spots' version of Eq. (7) of the main text. We see that, since $X_0 > 0$, the weak-coupling approximation favors the fully gapped chiral state, $(d_1, d_2) \sim (1, i)$.

3. Coupling between pairing potential and CDW fluctuations

In this section, we present the general expressions for the terms that describe the interplay between CDW fluctuations ϕ_i and SC order parameter d_i , see Eq. (A16). After straightforward calculation, we find:

$$\begin{aligned} \text{Tr} [(G_0 \Sigma_\Delta)^2 (G_0 \Sigma_\phi)^2] &= 8(\lambda T \Delta)^2 \sum_{\Omega, \mathbf{q}} |\phi_1(\Omega, \mathbf{q})|^2 \left[K_1(\Omega, \mathbf{q}) \left| \frac{\sqrt{3}}{2} d_1 - \frac{1}{2} d_2 \right|^2 + K_1(\Omega, -M\mathbf{q}) \left| \frac{\sqrt{3}}{2} d_1 + \frac{1}{2} d_2 \right|^2 \right] + \\ &+ |\phi_2(\Omega, \mathbf{q})|^2 \left[K_1(\Omega, -R_6 M \mathbf{q}) |d_2|^2 + K_1(\Omega, R_6^{-1} \mathbf{q}) \left| \frac{\sqrt{3}}{2} d_1 + \frac{1}{2} d_2 \right|^2 \right] + \\ &+ |\phi_3(\Omega, \mathbf{q})|^2 \left[K_1(\Omega, -R_6 \mathbf{q}) |d_2|^2 + K_1(\Omega, MR_6 \mathbf{q}) \left| \frac{\sqrt{3}}{2} d_1 - \frac{1}{2} d_2 \right|^2 \right], \end{aligned} \quad (\text{A19a})$$

$$\begin{aligned} \text{Tr} [(G_0 \Sigma_\Delta G_0 \Sigma_\phi)^2] &= -8(\lambda T \Delta)^2 \sum_{\Omega, \mathbf{q}} |\phi_1(\Omega, \mathbf{q})|^2 K_2(\Omega, \mathbf{q}) \left[-\frac{3}{2} |d_1|^2 + \frac{1}{2} |d_2|^2 \right] + \\ &+ |\phi_2(\Omega, \mathbf{q})|^2 K_2(\Omega, R_6^{-1} \mathbf{q}) \left[-|d_2|^2 - \frac{\sqrt{3}}{2} (d_1 d_2^* + d_2 d_1^*) \right] + |\phi_3(\Omega, \mathbf{q})|^2 K_2(\Omega, -R_6 \mathbf{q}) \left[-|d_2|^2 + \frac{\sqrt{3}}{2} (d_1 d_2^* + d_2 d_1^*) \right], \end{aligned} \quad (\text{A19b})$$

$$\begin{aligned} \text{Tr} [(G_0 \Sigma_\Delta)^4 (G_0 \Sigma_\phi)^2] &= -8(\lambda T \Delta^2)^2 \sum_{\Omega, \mathbf{q}} |\phi_1(\Omega, \mathbf{q})|^2 \left[K_3(\Omega, \mathbf{q}) \left| \frac{\sqrt{3}}{2} d_1 - \frac{1}{2} d_2 \right|^4 + K_3(\Omega, -M\mathbf{q}) \left| \frac{\sqrt{3}}{2} d_1 + \frac{1}{2} d_2 \right|^4 \right] + \\ &+ |\phi_2(\Omega, \mathbf{q})|^2 \left[K_3(\Omega, -R_6 M \mathbf{q}) |d_2|^4 + K_3(\Omega, R_6^{-1} \mathbf{q}) \left| \frac{\sqrt{3}}{2} d_1 + \frac{1}{2} d_2 \right|^4 \right] + \\ &+ |\phi_3(\Omega, \mathbf{q})|^2 \left[K_3(\Omega, -R_6 \mathbf{q}) |d_2|^4 + K_3(\Omega, MR_6 \mathbf{q}) \left| \frac{\sqrt{3}}{2} d_1 - \frac{1}{2} d_2 \right|^4 \right], \end{aligned} \quad (\text{A19c})$$

$$\begin{aligned} \text{Tr} [(G_0 \Sigma_\Delta)^2 (G_0 \Sigma_\Delta G_0 \Sigma_\phi)^2] &= 4(\lambda T \Delta^2)^2 \sum_{\Omega, \mathbf{q}} |\phi_1(\Omega, \mathbf{q})|^2 \left(-\frac{3}{2} |d_1|^2 + \frac{1}{2} |d_2|^2 \right) \times \\ &\times \left[K_4(\Omega, \mathbf{q}) \left| \frac{\sqrt{3}}{2} d_1 - \frac{1}{2} d_2 \right|^2 + K_4(\Omega, -M\mathbf{q}) \left| \frac{\sqrt{3}}{2} d_1 + \frac{1}{2} d_2 \right|^2 \right] + \\ &+ |\phi_2(\Omega, \mathbf{q})|^2 \left(-|d_2|^2 - \frac{\sqrt{3}}{2} (d_1 d_2^* + d_2 d_1^*) \right) \left[K_4(\Omega, -R_6 M \mathbf{q}) |d_2|^2 + K_4(\Omega, R_6^{-1} \mathbf{q}) \left| \frac{\sqrt{3}}{2} d_1 + \frac{1}{2} d_2 \right|^2 \right] + \\ &+ |\phi_3(\Omega, \mathbf{q})|^2 \left(-|d_2|^2 + \frac{\sqrt{3}}{2} (d_1 d_2^* + d_2 d_1^*) \right) \left[K_4(\Omega, -R_6 \mathbf{q}) |d_2|^2 + K_4(\Omega, MR_6 \mathbf{q}) \left| \frac{\sqrt{3}}{2} d_1 - \frac{1}{2} d_2 \right|^2 \right], \end{aligned} \quad (\text{A19d})$$

$$\begin{aligned} \text{Tr} [(G_0 \Sigma_\Delta G_0 \Sigma_\Delta G_0 \Sigma_\phi)^2] &= -16(\lambda T \Delta^2)^2 \sum_{\Omega, \mathbf{q}} |\phi_1(\Omega, \mathbf{q})|^2 K_5(\Omega, \mathbf{q}) \left| \frac{\sqrt{3}}{2} d_1 - \frac{1}{2} d_2 \right|^2 \left| \frac{\sqrt{3}}{2} d_1 + \frac{1}{2} d_2 \right|^2 + \\ &+ |\phi_2(\Omega, \mathbf{q})|^2 K_5(\Omega, R_6^{-1} \mathbf{q}) \left| \frac{\sqrt{3}}{2} d_1 + \frac{1}{2} d_2 \right|^2 |d_2|^2 + |\phi_3(\Omega, \mathbf{q})|^2 K_5(\Omega, -R_6 \mathbf{q}) \left| \frac{\sqrt{3}}{2} d_1 - \frac{1}{2} d_2 \right|^2 |d_2|^2, \end{aligned} \quad (\text{A19e})$$

where, again, R_6 is a six-fold rotation matrix, $M \equiv M_{12}$ is a mirror symmetry operation between hot spots 1 and 2, and we used the equalities $\xi_i(\mathbf{k}) = \xi_{i+1}(R_6 \mathbf{k})$ and $\xi_1(\mathbf{k}) = \xi_2(M\mathbf{k})$ in our derivation. Functions $K_1(\Omega, \mathbf{q}), \dots, K_5(\Omega, \mathbf{q})$ are defined as

$$\begin{aligned}
K_1(\Omega, \mathbf{q}) &\equiv \sum_{\mathbf{k}, \omega} \frac{\omega(\omega + \Omega) - \xi_{1\mathbf{k}}\xi_{2\mathbf{k}-\mathbf{q}}}{[\omega^2 + \xi_{1\mathbf{k}}^2]^2 [(\omega + \Omega)^2 + \xi_{2\mathbf{k}-\mathbf{q}}^2]}, \\
K_2(\Omega, \mathbf{q}) &\equiv \sum_{\mathbf{k}, \omega} \frac{1}{[\omega^2 + \xi_{1\mathbf{k}}^2] [(\omega + \Omega)^2 + \xi_{2\mathbf{k}-\mathbf{q}}^2]}, \\
K_3(\Omega, \mathbf{q}) &\equiv \sum_{\mathbf{k}, \omega} \frac{\omega(\omega + \Omega) - \xi_{1\mathbf{k}}\xi_{2\mathbf{k}-\mathbf{q}}}{[\omega^2 + \xi_{1\mathbf{k}}^2]^3 [(\omega + \Omega)^2 + \xi_{2\mathbf{k}-\mathbf{q}}^2]}, \\
K_4(\Omega, \mathbf{q}) &\equiv \sum_{\mathbf{k}, \omega} \frac{1}{[\omega^2 + \xi_{1\mathbf{k}}^2]^2 [(\omega + \Omega)^2 + \xi_{2\mathbf{k}-\mathbf{q}}^2]}, \\
K_5(\Omega, \mathbf{q}) &\equiv \sum_{\mathbf{k}, \omega} \frac{\omega(\omega + \Omega) - \xi_{1\mathbf{k}}\xi_{2\mathbf{k}-\mathbf{q}}}{[\omega^2 + \xi_{1\mathbf{k}}^2]^2 [(\omega + \Omega)^2 + \xi_{2\mathbf{k}-\mathbf{q}}^2]^2}. \tag{A20}
\end{aligned}$$

In our derivation, we also exploited the equalities $K_2(\Omega, -\mathbf{q}) = K_2(\Omega, M\mathbf{q})$ and $K_5(\Omega, -\mathbf{q}) = K_5(\Omega, M\mathbf{q})$.

The first two terms, (A19a)-(A19b), are given by diagrams in Figs. 4(a) and 4(b) and describe the Δ^2 correction to the CDW susceptibility. Terms (A19c)-(A19e) correspond to the Δ^4 correction to the CDW susceptibility, as represented by diagrams in Figs. 4(c)-4(e). We also note that all terms are expressed through fields $\phi_1 - \phi_3$ only, since $\phi_4 - \phi_6$ can be eliminated using equality $\phi_{i+3}(-\Omega, -\mathbf{q}) = [\phi_i(\Omega, \mathbf{q})]^*$.

Though functions $K_1 - K_5$ depend on the dispersion relations near hot spots, $\xi_{i\mathbf{k}}$, which we have not specified yet, a very general conclusion regarding the favorable superconducting state can be drawn without an explicit evaluation of K_i .

4. Feedback correction to free energy

Total free energy of CDW fluctuations in the presence of pairing is given by

$$F_{\text{CDW}} = -T \ln Z_{\text{CDW}}, \quad Z_{\text{CDW}} \equiv \int D\phi \exp[-(S_{\text{eff}} - S_{\Delta})], \tag{A21}$$

where we subtracted the weak-coupling contribution (A17).

Assuming that CDW fluctuations remain massive, we explicitly rewrite the effective action (A16) as a quadratic form of ϕ_i ,

$$S_{\text{eff}} - S_{\Delta} \approx T \sum_{i,j=1}^3 \sum_{\Omega, \mathbf{q}} \phi_i(\Omega, \mathbf{q}) \left\{ [\hat{V}^{-1}(\Omega, \mathbf{q})]^{ij} - \delta\chi^{ij}(\Omega, \mathbf{q}) \right\} \phi_j^*(\Omega, \mathbf{q}), \tag{A22}$$

where $\hat{V}(\Omega, \mathbf{q})$ is the normal-state bosonic propagator which includes the normal-state polarization operator, and $\delta\chi(\Omega, \mathbf{q})$ is a superconducting correction to the CDW susceptibility determined by Eqs. (A19a)-(A19e). Again, we expressed S_{eff} in terms of three independent complex fields $\phi_1(\Omega, \mathbf{q}) - \phi_3(\Omega, \mathbf{q})$ only.

Integrating out fields ϕ_i and expanding the result in powers of $\delta\chi$, or, equivalently, in powers of Δ , one easily obtains

$$F_{\text{CDW}} = F^{(0)} + \delta F_{\Delta}^{(2)} + \delta F_{\Delta}^{(4)} + \dots = F^{(0)} - T \text{Tr} \left(\hat{V} \delta\chi \right) - \frac{T}{2} \text{Tr} (\hat{V} \delta\chi)^2 + \dots, \tag{A23}$$

where \dots stands for the terms of order $O(\Delta^6)$.

The first term in Eq. (A23), $F^{(0)}$, does not depend on pairing potential and gives the energy of CDW fluctuations in the normal state. To evaluate second and third terms, we assume that the bosonic propagator is diagonal in patch space. Then, due to rotational symmetry, it has the form

$$\hat{V}(\Omega, \mathbf{q}) = \begin{pmatrix} V(\Omega, \mathbf{q}) & 0 & 0 \\ 0 & V(\Omega, R_6^{-1}\mathbf{q}) & 0 \\ 0 & 0 & V(\Omega, R_6^{-2}\mathbf{q}) \end{pmatrix}_{\text{patches}}. \tag{A24}$$

Assuming further that $V(\Omega, \mathbf{q})$ satisfies $V(\Omega, -M\mathbf{q}) = V(\Omega, \mathbf{q})$, we find for $\delta F_\Delta^{(2)}$

$$\begin{aligned} \delta F_\Delta^{(2)} &\equiv -T\text{Tr}(\hat{V}\delta\hat{\chi}) = 3(\lambda T\Delta)^2(4X_1 + X_2)(|d_1|^2 + |d_2|^2) - \\ &\quad - \frac{3(\lambda T\Delta^2)^2}{4} [(8X_3 + 4X_4 + 4X_5)(|d_1|^2 + |d_2|^2)^2 + (4X_3 + 2X_4 - X_5)|d_1^2 + d_2^2|^2], \end{aligned} \quad (\text{A25})$$

where we defined $X_i \equiv \sum_{\Omega, \mathbf{q}} V(\Omega, \mathbf{q})K_i(\Omega, \mathbf{q})$.

Analogously, using the equality $K_2(\Omega, -\mathbf{q}) = K_2(\Omega, M\mathbf{q})$, we find the expression for $\delta F_\Delta^{(4)}$

$$\delta F_\Delta^{(4)} \equiv -\frac{T}{2}\text{Tr}(\hat{V}\delta\hat{\chi})^2 = -\frac{3T^3(\lambda\Delta)^4}{2} [(|d_1|^2 + |d_2|^2)^2(Y_1 + 8Y_2 + 8Y_3 + 8Y_4) + |d_1^2 + d_2^2|^2(2Y_1 + 4Y_2 + 4Y_3 - 2Y_4)], \quad (\text{A26})$$

with

$$\begin{aligned} Y_1 &\equiv \sum_{\mathbf{q}, \Omega} V^2(\Omega, \mathbf{q})K_2^2(\Omega, \mathbf{q}), & Y_2 &\equiv \sum_{\mathbf{q}, \Omega} V^2(\Omega, \mathbf{q})K_1^2(\Omega, \mathbf{q}), \\ Y_3 &\equiv \sum_{\mathbf{q}, \Omega} V^2(\Omega, \mathbf{q})K_1(\Omega, \mathbf{q})K_2(\Omega, \mathbf{q}), & Y_4 &\equiv \sum_{\mathbf{q}, \Omega} V^2(\Omega, \mathbf{q})K_1(\Omega, \mathbf{q})K_1(\Omega, -M\mathbf{q}). \end{aligned} \quad (\text{A27})$$

It is straightforward to show that $Y_1 + Y_2 \geq 2|Y_3|$ and $Y_2 \geq |Y_4|$, which leads to $Y_1 + 2Y_2 + 2Y_3 - Y_4 \geq 0$. Hence, the correction to free energy $\delta F_\Delta^{(4)}$ *always* favors a nematic superconducting state. As we demonstrate below using specific examples, the correction $\delta F_\Delta^{(2)}$ becomes parametrically smaller than $\delta F_\Delta^{(4)}$ once the fluctuations become sufficiently strong.

If $V(\Omega, \mathbf{q})$ is strongly peaked at $\Omega = q = 0$, only the zeroth mode significantly contributes to free energy. In this case, the coupling between CDW fluctuations and SC order parameter is given by (we neglect $\phi^2 d^4$ terms for now)

$$\begin{aligned} S_{\phi-\Delta} &\approx \frac{1}{2}\text{Tr}[(G_0\Sigma_\Delta)^2(G_0\Sigma_\phi)^2] + \frac{1}{4}\text{Tr}[(G_0\Sigma_\Delta G_0\Sigma_\phi)^2] = \\ &= (\lambda T\Delta)^2 \{|\phi|^2|\mathbf{d}|^2[4K_1(0,0) + K_2(0,0)] + [P_1N_1 + P_2N_2][K_1(0,0) + K_2(0,0)]\}, \end{aligned} \quad (\text{A28})$$

in agreement with Eqs. (3) and (12) of the main text. Here we defined

$$\begin{aligned} |\phi|^2 &\equiv |\phi_1(0,0)|^2 + |\phi_2(0,0)|^2 + |\phi_3(0,0)|^2, & |\mathbf{d}|^2 &\equiv |d_1|^2 + |d_2|^2, \\ N_1 &\equiv |d_1|^2 - |d_2|^2, & N_2 &\equiv d_1d_2^* + d_2d_1^*, \\ P_1 &\equiv 2|\phi_1(0,0)|^2 - |\phi_2(0,0)|^2 - |\phi_3(0,0)|^2, & P_2 &\equiv \sqrt{3}(|\phi_2(0,0)|^2 - |\phi_3(0,0)|^2). \end{aligned} \quad (\text{A29})$$

Integrating out ϕ_i , we obtain

$$\delta F_\Delta^{(4)} \approx -\frac{3T^3(\lambda\Delta)^4}{2} \left[\int \frac{d^2q}{(2\pi)^2} V^2(0, q) \right] \left\{ [4K_1(0,0) + K_2(0,0)]^2 (|d_1|^2 + |d_2|^2)^2 + 2[K_1(0,0) + K_2(0,0)]^2 |d_1^2 + d_2^2|^2 \right\}, \quad (\text{A30})$$

in agreement with Eq. (4) of the main text. We see that the coupling between nematic bilinears N_iP_i is an essential ingredient that eventually leads to nematic superconductivity. As we demonstrate below within two explicit models, which we believe adequately describe the low-energy physics in twisted bilayer graphene at different dopings and twist angles, the quartic ($\sim \Delta^4$) term from $\delta F_\Delta^{(2)}$ (originating from the coupling $\phi^2 d^4$) becomes negligible compared to $\delta F_\Delta^{(4)}$ as the fluctuation strength increases.

5. Application for specific model: hot spots with linear dispersion

Now we explicitly calculate the feedback free energy for the model of twisted bilayer graphene with Fermi surface slightly away from the Van Hove singularity. In this case, the Fermi surface is shown in Fig. 3(b), with the single-electron dispersion near hot spots approximated by $\xi_i(\mathbf{k}) = v(\mathbf{k} \cdot \mathbf{n}_i)$, where \mathbf{n}_i is a unit vector in the ΓM_i direction. For concreteness, we choose the coordinates such that

$$\xi_1(\mathbf{k}) = -\frac{v}{2} \left(k_x + \sqrt{3}k_y \right), \quad \xi_2(\mathbf{k}) = -\frac{v}{2} \left(-k_x + \sqrt{3}k_y \right). \quad (\text{A31})$$

With these explicit expressions for $\xi_{i\mathbf{k}}$, we can calculate $K_i(\Omega, \mathbf{q})$ defined in Eq. (A20). Integrals over \mathbf{k} can be readily evaluated, giving

$$\begin{aligned} K_1(\Omega_m, \mathbf{q}) &= \frac{1}{4\sqrt{3}v^2} \frac{1}{(2\pi T)^2} \sum_n \frac{\text{sign}(n+1/2)\text{sign}(n+m+1/2)}{(n+1/2)^2} = \frac{1}{2\sqrt{3}v^2} \frac{1}{(2\pi T)^2} \psi'_0 \left(|m| + \frac{1}{2} \right), \\ K_2(\Omega_m, \mathbf{q}) &= \frac{1}{2\sqrt{3}v^2} \frac{1}{(2\pi T)^2} \sum_n \frac{1}{|n+1/2||n+m+1/2|} = \frac{1}{2\sqrt{3}v^2} \frac{1}{(2\pi T)^2} \begin{cases} 4 \left[\psi_0 \left(|m| + \frac{1}{2} \right) - \psi_0 \left(\frac{1}{2} \right) \right] / |m|, & m \neq 0 \\ \pi^2, & m = 0 \end{cases}, \\ K_3(\Omega_m, \mathbf{q}) &= \frac{\sqrt{3}}{16v^2} \frac{1}{(2\pi T)^4} \sum_n \frac{\text{sign}(n+1/2)\text{sign}(n+m+1/2)}{(n+1/2)^4}, \\ K_4(\Omega_m, \mathbf{q}) &= \frac{1}{4\sqrt{3}v^2} \frac{1}{(2\pi T)^4} \sum_n \frac{1}{|n+1/2|^3 |n+m+1/2|}, \\ K_5(\Omega_m, \mathbf{q}) &= \frac{1}{8\sqrt{3}v^2} \frac{1}{(2\pi T)^4} \sum_n \frac{\text{sign}(n+1/2)\text{sign}(n+m+1/2)}{(n+1/2)^2 (n+m+1/2)^2}. \end{aligned} \quad (\text{A32})$$

Here $\psi_0(x)$ is the digamma function, and $\Omega_m = 2\pi Tm$. In principle, frequency dependence of $K_3 - K_5$ can also be expressed through ψ_0 and its derivatives. The resulting expressions, however, are rather cumbersome, and we do not present them here.

To calculate the explicit expression for the feedback free energy, we further assume that the bosonic propagator is given by

$$V(\Omega_m, \mathbf{q}) = \frac{\chi_0}{c(q_0^2 + q^2) + \Omega_m^2}, \quad \text{with} \quad T \ll cq_0 \ll ck_{\max}, \quad (\text{A33})$$

where k_{\max} is an ultraviolet momentum cutoff corresponding to the size of patches.

Corrections X_1 and X_2 in Eq. (A25) only shift T_c , so we do not consider them here. Then, it can be directly shown that the most singular contribution to $\delta F_\Delta^{(2)}$ comes from X_4 , since $K_4(\Omega_m, \mathbf{q}) \sim 1/m$ for $m \gg 1$. Consequently, omitting terms $\sim \Delta^2$, we find for $\delta F_\Delta^{(2)}$

$$\delta F_\Delta^{(2)} \rightarrow -\frac{3(\lambda T \Delta^2)^2}{2} X_4 [2(|d_1|^2 + |d_2|^2)^2 + |d_1^2 + d_2^2|^2], \quad X_4 = \frac{7\zeta(3)}{4\sqrt{3}\pi} \left(\frac{1}{2\pi T} \right)^4 \frac{\chi_0}{c^2 v^2} \ln \frac{k_{\max}}{q_0} \ln \frac{c^2 k_{\max} q_0}{T^2}. \quad (\text{A34})$$

Analogously, performing integration over \mathbf{q} and summation over Ω_m , we find

$$Y_1 = 3.23 \left(\frac{\chi_0}{q_0 v^2 c^2} \right)^2 \cdot \left(\frac{1}{2\pi T} \right)^4, \quad Y_2 = Y_4 = 0.18 \left(\frac{\chi_0}{q_0 v^2 c^2} \right)^2 \cdot \left(\frac{1}{2\pi T} \right)^4, \quad Y_3 = 0.54 \left(\frac{\chi_0}{q_0 v^2 c^2} \right)^2 \cdot \left(\frac{1}{2\pi T} \right)^4, \quad (\text{A35})$$

leading to

$$\delta F_\Delta^{(4)} = -\frac{13.46}{(2\pi)^4} \left(\frac{\chi_0 T \lambda^2}{q_0 v^2 c^2} \right)^2 \frac{\Delta^4}{T^3} [1.16(|d_1|^2 + |d_2|^2)^2 + |d_1^2 + d_2^2|^2]. \quad (\text{A36})$$

This result is presented in Eq. (13) of the main text. We see that $\delta F_\Delta^{(4)}$ becomes dominant over $\delta F_\Delta^{(2)}$ (at fourth-order in Δ) when fluctuations become sufficiently strong, i.e., when q_0 becomes sufficiently small. This observation allows us to focus on the $\delta F_\Delta^{(4)}$ term in this paper.

6. Application for specific model: hot spots at Van Hove singularities

Next, we consider a model of twisted bilayer graphene with the filling factor close to $n = 2$ electron/holes per supercell. In this case, hot spots coincide with the Van Hove singularities, and the representative Fermi surface is shown in Fig. 3(c). We assume for simplicity that the dispersion near Van Hove points is the same as in the case of monolayer graphene, i.e., $\xi_{1,2}(\mathbf{k}) = 3t(k_y^2 \pm \sqrt{3}k_x k_y)/2$, where t is an effective hopping constant, and the

hyperlattice constant is absorbed into the definition of t . While we consider sufficiently strong CDW fluctuations, we stay away from the immediate vicinity of the transition into the CDW-ordered state. Hence, we assume that the CDW propagator is given by

$$V(\Omega, q) = \frac{\chi_0}{c^2(q_0^2 + q^2)}, \quad T/tk_{\max} \ll q_0 \ll \sqrt{T/t}, \quad (\text{A37})$$

where, again, k_{\max} is an effective ultraviolet momentum cutoff. The relevant bosonic momenta and frequencies then satisfy $q \lesssim \sqrt{T/t}$ and $\Omega \sim T$, respectively. In this range of frequencies and momenta, the asymptotic behavior of functions $K_i(\Omega, \mathbf{q})$ defined in Eq. (A20) is given by

$$K_i(\Omega, \mathbf{q}) = \frac{1}{3\sqrt{3}\pi t} f_i(\Omega) \ln \left(\min \left\{ k_{\max} \sqrt{\frac{t}{T}}, \frac{1}{|q_y|} \sqrt{\frac{T}{t}} \right\} \right), \quad q \lesssim \sqrt{\frac{T}{t}}, \quad \Omega \sim T. \quad (\text{A38})$$

The main contribution to K_i comes from the 'nesting' direction, $k_y \approx 0$. Frequency-dependent functions $f_i(\Omega)$ are given by

$$\begin{aligned} f_1(\Omega_m) &= \frac{1}{2} \sum_{\omega_n} \frac{2 + 2\text{sign}[\omega_n(\omega_n + \Omega_m)] + \frac{\Omega_m}{\omega_n}}{|\omega_n|(|\omega_n| + |\omega_n + \Omega_m|)^2} = \frac{1}{(2\pi T)^3} \cdot \begin{cases} 0, & m \neq 0, \\ 7\zeta(3), & m = 0 \end{cases} \\ f_2(\Omega_m) &= \sum_{\omega_n} \frac{1}{|\omega_n||\omega_n + \Omega_m|(|\omega_n| + |\omega_n + \Omega_m|)} = \frac{1}{(2\pi T)^3} \cdot \begin{cases} \frac{4}{m^2} \left[\ln 4 + \text{HarmonicNumber} \left(\frac{|m|-1}{2} \right) \right], & m \neq 0, \\ 7\zeta(3), & m = 0 \end{cases} \\ f_3(\Omega_m) &= \frac{1}{8} \sum_{\omega_n} \frac{3\omega_n^2 + |\omega_n(\omega_n + \Omega_m)| + \text{sign}[\omega_n(\omega_n + \Omega_m)] \cdot [8\omega_n^2 + 9|\omega_n(\omega_n + \Omega_m)| + 3(\omega_n + \Omega_m)^2]}{\omega_n^4(|\omega_n| + |\omega_n + \Omega_m|)^3} = \\ &= \frac{1}{(2\pi T)^5} \begin{cases} -\frac{1}{4m^2} \left[\psi_0'' \left(\frac{1+|m|}{2} \right) + 14\zeta(3) \right], & m \neq 0, \\ 93\zeta(5)/4, & m = 0 \end{cases} \\ f_4(\Omega_m) &= \frac{1}{2} \sum_{\omega_n} \frac{2|\omega_n| + |\omega_n + \Omega_m|}{|\omega_n|^3 |\omega_n + \Omega_m| (|\omega_n| + |\omega_n + \Omega_m|)^2} = \\ &= \frac{1}{(2\pi T)^5} \cdot \begin{cases} \frac{1}{m^4} \left[8 \ln 2 + 4\text{HarmonicNumber} \left(\frac{|m|-1}{2} \right) + 7m^2\zeta(3) \right], & m \neq 0, \\ 93\zeta(5)/4, & m = 0 \end{cases}, \\ f_5(\Omega_m) &= \frac{1}{2} \sum_{\omega_n} \frac{|\omega_n||\omega_n + \Omega_m| + \text{sign}[\omega_n(\omega_n + \Omega_m)] \cdot [\omega_n^2 + 3|\omega_n(\omega_n + \Omega_m)| + (\omega_n + \Omega_m)^2]}{\omega_n^2(\omega_n + \Omega_m)^2(|\omega_n| + |\omega_n + \Omega_m|)^3} = \\ &= \frac{1}{(2\pi T)^5} \begin{cases} \frac{1}{2m^4} \left[m^2\psi_0'' \left(2, \frac{1+|m|}{2} \right) - 8\text{HarmonicNumber} \left(\frac{|m|-1}{2} \right) - 16 \ln 2 \right], & m \neq 0, \\ 93\zeta(5)/4, & m = 0 \end{cases} \end{aligned} \quad (\text{A39})$$

where, again, $\omega_n = 2\pi T(n+1/2)$, $\Omega_m = 2\pi Tm$, $\zeta(x)$ is the Riemann zeta function, and $\psi_0(x)$ is the digamma function. After straightforward integration over \mathbf{q} and summation over Ω_m , we find

$$\begin{aligned} X_1 &= \frac{7\zeta(3)}{273\sqrt{3}\pi^5} \frac{\chi_0}{tc^2T^3} \ln^2 \frac{T}{tq_0^2}, & X_2 &= 4 \frac{7\zeta(3)}{273\sqrt{3}\pi^5} \frac{\chi_0}{tc^2T^3} \ln^2 \frac{T}{tq_0^2} = 4X_1, \\ X_3 &= \frac{23.22}{2^{10}3\sqrt{3}\pi^7} \frac{\chi_0}{tc^2T^5} \ln^2 \frac{T}{tq_0^2}, & X_4 &= \frac{128.58}{2^{10}3\sqrt{3}\pi^7} \frac{\chi_0}{tc^2T^5} \ln^2 \frac{T}{tq_0^2}, \\ X_5 &= \frac{17.85}{2^{10}3\sqrt{3}\pi^7} \frac{\chi_0}{tc^2T^5} \ln^2 \frac{T}{tq_0^2}, \\ Y_1 &= \frac{144.57}{2^{10}3^3\pi^9} \frac{\chi_0^2}{t^2c^4q_0^2T^6} \ln^2 \frac{T}{tq_0^2}, & Y_2 = Y_3 = Y_4 &= \frac{49\zeta^2(3)}{2^{10}3^3\pi^9} \frac{\chi_0^2}{t^2c^4q_0^2T^6} \ln^2 \frac{T}{tq_0^2} \approx \frac{70.8}{2^{10}3^3\pi^9} \frac{\chi_0^2}{t^2c^4q_0^2T^6} \ln^2 \frac{T}{tq_0^2}. \end{aligned} \quad (\text{A40})$$

Collecting everything together, we find the feedback correction to free energy:

$$\delta F_{\Delta}^{(2)} \approx \frac{7\zeta(3)}{2^4\sqrt{3}\pi^5} \frac{\chi_0\lambda^2}{tc^2} \frac{\Delta^2}{T} \ln^2 \frac{T}{tq_0^2} (|d_1|^2 + |d_2|^2) - \frac{6.0}{(2\pi)^7} \frac{\chi_0\lambda^2}{tc^2} \frac{\Delta^4}{T^3} \ln^2 \frac{T}{tq_0^2} [2.32(|d_1|^2 + |d_2|^2)^2 + |d_1^2 + d_2^2|^2], \quad (\text{A41})$$

$$\delta F_{\Delta}^{(4)} \approx -\frac{3.16}{(2\pi)^8} \left(\frac{\chi_0 \lambda^2}{t q_0 c^2}\right)^2 \frac{\Delta^4}{T^3} \ln^2 \frac{T}{t q_0^2} [2.58(|d_1|^2 + |d_2|^2)^2 + |d_1^2 + d_2^2|^2]. \quad (\text{A42})$$

We see, again, that $\delta F_{\Delta}^{(4)}$ becomes more significant than the fourth-order term in $\delta F_{\Delta}^{(2)}$ as q_0 decreases, hence, the latter can be neglected when fluctuations become sufficiently strong.

Appendix B: Nematic d -wave superconductivity in presence of spin density wave fluctuations

In this appendix, we repeat the analysis of the previous appendix for the case of two-component d -wave superconductor coupled to spin density wave fluctuations, instead of charge density wave. Due to spin-rotation invariance, it is sufficient to consider the case of uniaxial SDW only, which we do for simplicity. The answer for the feedback free energy in case of $SU(2)$ -symmetric SDW is given by the same expression, up to an overall numerical coefficient.

The whole analysis for the case of SDW fluctuations is very similar to the one presented in the previous section. The only difference is that the coupling between fermions and SDW fluctuations is now given by

$$\begin{aligned} S_{\psi-\phi} &= \lambda T^2 \sum_{\alpha, \beta=\uparrow, \downarrow} \sum_{i=1}^6 \sum_{\omega_n, \Omega_m} \sum_{\mathbf{k}, \mathbf{q}} \psi_{i+1\alpha}^{\dagger}(\omega_n + \Omega_m, \mathbf{k} + \mathbf{q}) \sigma_{\alpha\beta}^z \psi_{i\beta}(\omega_n, \mathbf{k}) \phi_i(\Omega_m, \mathbf{q}) + \text{H. c.} = \\ &= T \sum_{\alpha, \beta=\uparrow, \downarrow} \sum_{i, j=1}^6 \sum_{\omega_n, \Omega_m} \sum_{\mathbf{k}, \mathbf{q}} \psi_{i\alpha}^{\dagger}(\omega_n + \Omega_m, \mathbf{k} + \mathbf{q}) \psi_{j\beta}(\omega_n, \mathbf{k}) \hat{\Sigma}_{ij, \alpha\beta}(\Omega_m, \mathbf{q}), \end{aligned} \quad (\text{B1})$$

with $\hat{\Sigma}(\mathbf{q}, \Omega)$ defined as

$$\hat{\Sigma}_{ij, \alpha\beta}(\Omega, \mathbf{q}) = \lambda T \cdot \sigma_{\alpha\beta}^z \otimes \begin{pmatrix} 0 & \phi_4(\Omega, \mathbf{q}) & 0 & 0 & 0 & \phi_6(\Omega, \mathbf{q}) \\ \phi_1(\Omega, \mathbf{q}) & 0 & \phi_5(\Omega, \mathbf{q}) & 0 & 0 & 0 \\ 0 & \phi_2(\Omega, \mathbf{q}) & 0 & \phi_6(\Omega, \mathbf{q}) & 0 & 0 \\ 0 & 0 & \phi_3(\Omega, \mathbf{q}) & 0 & \phi_1(\Omega, \mathbf{q}) & 0 \\ 0 & 0 & 0 & \phi_4(\Omega, \mathbf{q}) & 0 & \phi_2(\Omega, \mathbf{q}) \\ \phi_3(\Omega, \mathbf{q}) & 0 & 0 & 0 & \phi_5(\Omega, \mathbf{q}) & 0 \end{pmatrix}_{ij}, \quad (\text{B2})$$

instead of Eqs. (A6)-(A7), and σ^z is a Pauli matrix in spin space. This leads to the self-energy in the Nambu space

$$\Sigma_{\phi}(\Omega, \mathbf{q}) = \hat{\Sigma}(\Omega, \mathbf{q}) \otimes I_N, \quad (\text{B3})$$

instead of the corresponding term in Eq. (A10).

As a consequence of a different structure of Σ_{ϕ} in Nambu space, the expressions for $\text{Tr}[(G_0 \Sigma_{\Delta} G_0 \Sigma_{\phi})^2]$ and $\text{Tr}[(G_0 \Sigma_{\Delta})^2 (G_0 \Sigma_{\Delta} G_0 \Sigma_{\phi})^2]$ in Eqs. (A19b) and (A19d) contain an overall extra minus sign compared to the case of CDW fluctuations, which can be absorbed by redefining $K_2 \rightarrow -K_2$ and $K_4 \rightarrow -K_4$. This leads, in particular, to an extra minus sign in front of terms in free energy containing X_2 , X_4 , and Y_3 . More explicitly, the feedback corrections in case of SDW fluctuations are given by

$$\begin{aligned} \delta F_{\Delta}^{(2)} &= 3(\lambda T \Delta)^2 (4X_1 - X_2)(|d_1|^2 + |d_2|^2) - \\ &\quad - \frac{3(\lambda T \Delta^2)^2}{4} [(8X_3 - 4X_4 + 4X_5)(|d_1|^2 + |d_2|^2)^2 + (4X_3 - 2X_4 - X_5)|d_1^2 + d_2^2|^2], \end{aligned} \quad (\text{B4})$$

$$\delta F_{\Delta}^{(4)} = -\frac{3T^3(\lambda\Delta)^4}{2} \left[(|d_1|^2 + |d_2|^2)^2 (Y_1 + 8Y_2 - 8Y_3 + 8Y_4) + |d_1^2 + d_2^2|^2 (2Y_1 + 4Y_2 - 4Y_3 - 2Y_4) \right], \quad (\text{B5})$$

where, again, $X_i \equiv \sum_{\Omega, \mathbf{q}} V(\Omega, \mathbf{q}) K_i(\Omega, \mathbf{q})$, and K_i, Y_i are defined in Eqs. (A20) and (A27).

Similarly to the case of CDW fluctuations, the contribution $\delta F_{\Delta}^{(4)}$ always favors the nematic superconducting state, hence, the main result of our paper remains valid for SDW fluctuations as well. The absolute value of this correction, however, is smaller because of a minus sign in front of Y_3 . The quartic term in $\delta F_{\Delta}^{(2)}$, on the other hand, changes its

sign within the specific models for twisted bilayer graphene we considered in Appendices A 5 and A 6. This happens because of an additional minus sign in front of X_4 . Hence, $\delta F_{\Delta}^{(2)}$ favors chiral state in case of SDW fluctuations. At sufficiently strong fluctuations, however, the fourth-order term in $\delta F_{\Delta}^{(2)}$ is parametrically smaller than $\delta F_{\Delta}^{(4)}$ and thus can be neglected again, justifying our conclusion about the stability of nematic superconductivity.

-
- ¹ Y. Cao, V. Fatemi, S. Fang, K. Watanabe, T. Taniguchi, E. Kaxiras, and P. Jarillo-Herrero, *Nature (London)* **556**, 43 (2018).
 - ² Yuan Cao, Noah F. Q. Yuan, Daniel Rodan-Legrain, Oriol Rubies-Bigorda, Kenji Watanabe, Takashi Taniguchi, Liang Fu, and Pablo Jarillo-Herrero, In preparation.
 - ³ K. Matano, M. Kriener, K. Segawa, Y. Ando, and Guoqing Zheng, *Nat. Phys.* **12**, 852 (2016).
 - ⁴ S. Yonezawa, K. Tajiri, S. Nakata, Y. Nagai, Z. Wang, K. Segawa, Y. Ando, and Y. Maeno, *Nat. Phys.* **17**, 123-126 (2017).
 - ⁵ Kristin Willa, Roland Willa, Kok Wee Song, G. D. Gu, John A. Schneeloch, Ruidan Zhong, Alexei E. Koshelev, Wai-Kwong Kwok, and Ulrich Welp, *Phys. Rev. B* **98**, 184509 (2018).
 - ⁶ Y. Pan, A. M. Nikitin, G. K. Araizi, Y. K. Huang, Y. Matsushita, T. Naka, and A. de Visser, *Sci. Rep.* **6**, 28632 (2016).
 - ⁷ A. M. Nikitin, Y. Pan, Y. K. Huang, T. Naka, and A. de Visser, *Phys. Rev. B* **94**, 144516 (2016).
 - ⁸ J. Shen, W.-Y. He, N. F. Q. Yuan, Z. Huang, C.-w. Cho, S. H. Lee, Y. S. Hor, K. T. Law, and R. Lortz, *npj Quantum Materials* **2**, 59 (2017).
 - ⁹ Tomoya Asaba, B. J. Lawson, Colin Tinsman, Lu Chen, Paul Corbae, Gang Li, Y. Qiu, Y. S. Hor, Liang Fu, and Lu Li, *Phys. Rev. X* **7**, 011009 (2017).
 - ¹⁰ Ran Tao, Ya-Jun Yan, Xi Liu, Zhi-Wei Wang, Yoichi Ando, Tong Zhang, and Dong-Lai Feng, *Phys. Rev. X* **8**, 041024 (2018).
 - ¹¹ Liang Fu, *Phys. Rev. B* **90**, 100509(R) (2014).
 - ¹² Liang Fu and Erez Berg, *Phys. Rev. Lett.* **105**, 097001 (2010).
 - ¹³ Jörn W. F. Venderbos, Vladyslav Kozii, Liang Fu, *Phys. Rev. B* **94**, 180504(R) (2016).
 - ¹⁴ F. Wu and I. Martin, *Phys. Rev. B* **96**, 144504 (2017).
 - ¹⁵ Z. Liu, X. Yao, J. Shao, M. Zuo, L. Pi, S. Tan, C. Zhang, and Y. Zhang, *J. Am. Chem. Soc.*, **137** (33), 10512 (2015).
 - ¹⁶ H. Leng, D. Cherian, Y. K. Huang, J.-C. Orain, A. Amato, and A. de Visser *Phys. Rev. B* **97**, 054503 (2018).
 - ¹⁷ M. P. Smylie, H. Claus, U. Welp, W.-K. Kwok, Y. Qiu, Y. S. Hor, and A. Snezhko, *Phys. Rev. B* **94**, 180510(R) (2016).
 - ¹⁸ M. P. Smylie, K. Willa, H. Claus, A. Snezhko, I. Martin, W.-K. Kwok, Y. Qiu, Y. S. Hor, E. Bokari, P. Niraula, A. Kayani, V. Mishra, and U. Welp, *Phys. Rev. B* **96**, 115145 (2017).
 - ¹⁹ M. P. Smylie, K. Willa, K. Ryan, H. Claus, W.-K. Kwok, Y. Qiu, Y. S. Hor, and U. Welp *Physica C* **543**, 58-61 (2017).
 - ²⁰ Jörn W. F. Venderbos, Vladyslav Kozii, Liang Fu, *Phys. Rev. B* **94**, 094522 (2016).
 - ²¹ A. A. Zyuzin, J. Garaud, and E. Babaev, *Phys. Rev. Lett.* **119**, 167001 (2017).
 - ²² F. Wu and I. Martin, *Phys. Rev. B* **95**, 224503 (2017).
 - ²³ Matthias Hecker and Jörg Schmalian, *npj Quantum Materials* **3**, 26 (2018).
 - ²⁴ Wen Huang and Hong Yao, *Phys. Rev. Lett.* **121**, 157002 (2018).
 - ²⁵ Hiroki Uematsu, Takeshi Mizushima, Atsushi Tsuruta, Satoshi Fujimoto, and J. A. Sauls, arXiv:1809.06989.
 - ²⁶ Annica M. Black-Schaffer and Sebastian Doniach, *Phys. Rev. B* **75**, 134512 (2007).
 - ²⁷ M. Cheng, K. Sun, V. Galitski, and S. Das Sarma, *Phys. Rev. B* **81**, 024504 (2010).
 - ²⁸ Luca Chirolli, *Phys. Rev. B* **98**, 014505 (2018).
 - ²⁹ R. Nandkishore, L. S. Levitov, and A. V. Chubukov, *Nat. Phys.* **8**, 158 (2012).
 - ³⁰ R. Nandkishore, R. Thomale, and A. V. Chubukov, *Phys. Rev. B* **89**, 144501 (2014).
 - ³¹ P. W. Anderson and W. F. Brinkman, *Phys. Rev. Lett.* **30**, 1108 (1973).
 - ³² W. F. Brinkman, J. W. Serene, and P. W. Anderson, *Phys. Rev. A* **10**, 2386 (1974).
 - ³³ A. J. Leggett, *Rev. Mod. Phys.* **47**, 331 (1975).
 - ³⁴ Y. Cao, V. Fatemi, A. Demir, S. Fang, S. L. Tomarken, J. Y. Luo, J. D. Sanchez-Yamagishi, K. Watanabe, T. Taniguchi, E. Kaxiras, R. C. Ashoori, and P. Jarillo-Herrero, *Nature (London)* **556**, 80 (2018).
 - ³⁵ Matthew Yankowitz, Shaowen Chen, Hryhoriy Polshyn, K. Watanabe, T. Taniguchi, David Graf, Andrea F. Young, and Cory R. Dean, *Science* **363**, 1059 (2019).
 - ³⁶ H. Isobe, N. F. Q. Yuan, and L. Fu, *Phys. Rev. X* **8**, 041041 (2018).
 - ³⁷ C. Xu and L. Balents, *Phys. Rev. Lett.* **121**, 087001 (2018).
 - ³⁸ Yi-Zhuang You and Ashvin Vishwanath, arXiv:1805.06867.
 - ³⁹ Guo-Yi Zhu, Tao Xiang, and Guang-Ming Zhang, arXiv:1806.07535.
 - ⁴⁰ John F. Dodaro, Steven A. Kivelson, Yoni Schattner, Xiao-Qi Sun, and Chao Wang, *Phys. Rev. B* **98**, 075154 (2018).
 - ⁴¹ E. Laksonoa, J. N. Leawa, A. Reavesc, M. Singhc, X. Wanga, S. Adama, and X. Gu, *Solid State Commun.* **282**, 38 (2018).
 - ⁴² G. E. Volovik, *Pisma ZhETF* **107**, 537-538 (2018) [*JETP Letters* **107**, 516-517 (2018)].
 - ⁴³ Hoi Chun Po, Liuju Zou, Ashvin Vishwanath, and T. Senthil, *Phys. Rev. X* **8**, 031089 (2018).
 - ⁴⁴ Ganapathy Baskaran, arXiv:1804.00627
 - ⁴⁵ B. Padhi, C. Setty, and P. W. Phillips, *Nano Lett.* **18**, 6175 (2018).
 - ⁴⁶ Bikash Padhi and Philip Phillips, arXiv:1810.00884.
 - ⁴⁷ Kyungmin Lee, Tamaghna Hazra, Mohit Randeria, and Nandini Trivedi, arXiv:1806.08795.
 - ⁴⁸ C.-C. Liu, L.-D. Zhang, W.-Q. Chen, and F. Yang, *Phys. Rev. Lett.* **121**, 217001 (2018).
 - ⁴⁹ Francisco Guinea and Niels R. Walet, *PNAS* **115**, 13174 (2018).

- ⁵⁰ Stephen Carr, Shiang Fang, Pablo Jarillo-Herrero, and Efthimios Kaxiras, Phys. Rev. B **98**, 085144 (2018)
- ⁵¹ J. Gonzalez and T. Stauber, Phys. Rev. Lett. **122**, 026801 (2019).
- ⁵² Yury Sherkunov and Joseph J. Betouras, Phys. Rev. B **98**, 205151 (2018).
- ⁵³ Biao Lian, Zhijun Wang, and B. Andrei Bernevig, arXiv:1807.04382
- ⁵⁴ Ying Su and Shi-Zeng Lin, Phys. Rev. B **98**, 195101 (2018).
- ⁵⁵ Jörn W. F. Venderbos, Rafael M. Fernandes, Phys. Rev. B **98**, 245103 (2018).
- ⁵⁶ Xiao-Chuan Wu, Kelly Ann Pawlak, Chao-Ming Jian, and Cenke Xu, arXiv:1805.06906.
- ⁵⁷ Fengcheng Wu, A. H. MacDonald, and Ivar Martin, Phys. Rev. Lett. **121**, 257001 (2018).
- ⁵⁸ Yu-Ping Lin and Rahul M. Nandkishore, Phys. Rev. B **98**, 214521 (2018).
- ⁵⁹ Masayuki Ochi, Mikito Koshino, and Kazuhiko Kuroki, Phys. Rev. B **98**, 081102(R) (2018).
- ⁶⁰ Liang Chen, Hui-Zhen Li, and Rong-Sheng Han, J. Phys.: Condens. Matter **31**, 065601 (2019).
- ⁶¹ Q.-K. Tang, L. Yang, D. Wang, F.-C. Zhang, and Q.-H. Wang, Phys. Rev. B **99**, 094521 (2019).
- ⁶² Young Woo Choi and Hyoung Joon Choi, Phys. Rev. B **98**, 241412(R) (2018).
- ⁶³ Rafael M. Fernandes and Andrew J. Millis, Phys. Rev. Lett. **111**, 127001 (2013).
- ⁶⁴ Youngwook Kim, Patrick Herlinger, Pilkyung Moon, Mikito Koshino, Takashi Taniguchi, Kenji Watanabe, and Jürgen H. Smet, Nano Lett. **16** (**8**), pp 5053-5059 (2016).
- ⁶⁵ M. Tinkham, *Introduction to Superconductivity* 2nd ed. (McGraw-Hill Book Co., New York, 1996).
- ⁶⁶ Rafael M. Fernandes, Peter P. Orth, and Jörg Schmalian, Ann. Rev. Cond. Matt. Phys. **10**, 133 (2019).